VIP *The following Communications have been judged by at least two referees to be "very important papers" and will be published online at www.angewandte.org soon:*

*X. Xin, M. He, W. Han, J. Jung, Z. Lin**
Low-Cost Counter Electrodes for High-Efficiency Dye-Sensitized Solar Cells

*M. E. Weiss, E. M. Carreira**
Total Synthesis of (+)-Daphmanidin E

*J. Bacsa, F. Hanke, S. Hindley, R. Odrea, G. R. Darling, A. C. Jones, A. Steiner**
The Solid-State Structures of Dimethylzinc and Diethylzinc

Z.-C. Wang, N. Dietl, R. Kretschmer, T. Weiske, M. Schlangen, H. Schwarz**
Catalytic Redox Reactions in the CO/N$_2$O System Mediated by the Bimetallic Oxide-Cluster Couple AlVO$_3^+$/AlVO$_4^+$

*C. D. N. Gomes, O. Jacquet, C. Villiers, P. Thuéry, M. Ephritikhine, T. Cantat**
A Diagonal Approach to Chemical Recycling of Carbon Dioxide: New Organocatalytic Transformation for the Reductive Functionalization of CO$_2$

*X. Zhang, T. J. Emge, K. C. Hultzsch**
A Chiral Phenoxyamine Magnesium Catalyst for the Enantioselective Hydroamination/Cyclization of Aminoalkenes and Intermolecular Hydroamination of Vinyl Arenes

H. Qin, P. Gao, F. Wang, L. Zhao, J. Zhu, A. Wang, T. Zhang, R. Wu, H. Zou**
Highly Efficient Extraction of Serum Peptides by Ordered Mesoporous Carbon

Author Profile

"The biggest challenge facing scientists is the molecular basis of consciousness.
My favorite quote is "Never publish faster than you think" (Prof. P. M. Etxenike) …"
This and more about Fernando P. Cossío can be found on page 11038.

News

F. Glorius

X. Hu

M. Drieß

K. Gademann

Obituaries

Books

Contents

Highlights

Asymmetric Dihalogenation

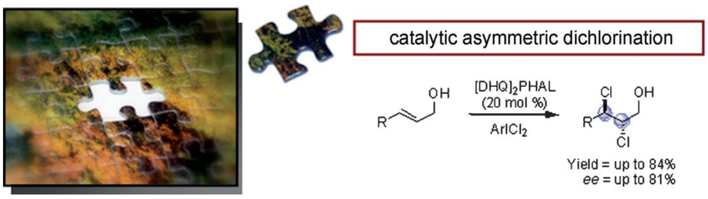

The missing piece: The long-pursued asymmetric catalytic dichlorination reaction has recently been reported (see scheme). The multiple issues faced to develop such an elusive target are discussed.

Tishchenko Reaction

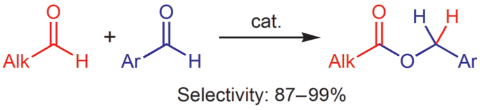

A sustainable synthesis of esters? The recent report of the selective intermolecular crossed-Tishchenko reaction is a major advancement of this textbook reaction. In the presence of a Ni–NHC catalyst (NHC = N-heterocyclic carbene), various benzyl esters of aliphatic acids can be synthesized with perfect atom economy from 1:1 mixtures of aromatic and aliphatic aldehydes.

Minireviews

Inorganic Synthesis

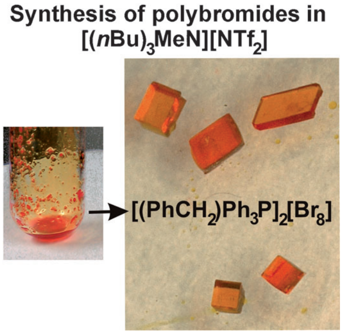

What can ionic liquids contribute to the synthesis of inorganic compounds? As a result of the low vapor pressure, wide temperature range over which they are liquid, their weak coordination properties, and high thermal stability, ionic liquids allow for the synthesis of several new compounds. The picture shows one of the first examples; more is to be discovered in the Minireview.

For the USA and Canada: ANGEWANDTE CHEMIE International Edition (ISSN 1433-7851) is published weekly by Wiley-VCH, PO Box 191161, 69451 Weinheim, Germany. Air freight and mailing in the USA by Publications Expediting Inc., 200 Meacham Ave., Elmont, NY 11003. Periodicals postage paid at Jamaica, NY 11431. US POSTMASTER: send address changes to *Angewandte Chemie*, Journal Customer Services, John Wiley & Sons Inc., 350 Main St., Malden, MA 02148-5020. Annual subscription price for institutions: US$ 11.738/10.206 (valid for print and electronic / print or electronic delivery); for individuals who are personal members of a national chemical society prices are available on request. Postage and handling charges included. All prices are subject to local VAT/ sales tax.

Reviews

Aerobic Oxidations

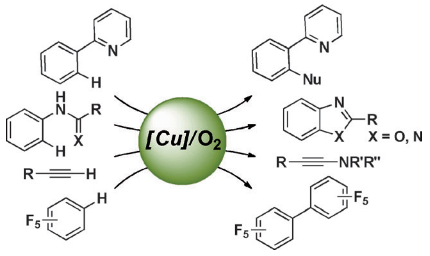

The rapid recent growth of Cu-catalyzed aerobic oxidative C–H functionalization reactions belies the extensive history of such transformations, which can be traced to the discovery of alkyne coupling reactions by Glaser in the 19th century. Recent studies implicate multiple possible mechanisms for these reactions, ranging from classical single-electron-transfer pathways to the involvement of novel organometallic intermediates.

Communications

α-Ketoamides

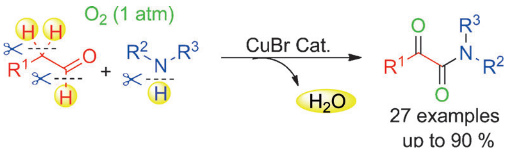

Efficient and practical: The title reaction provides an efficient route to α-ketoamides compounds, which are ubiquitous structural units in a number of biologically active compounds. N-substituted anilines are suitable substrates for this transformation. Two C_{sp^3}–H bonds as well as one C_{sp^2}–H and one N–H bond are cleaved in this reaction. Molecular oxygen (1 atm) is used as the oxidant and the reaction involves dioxygen activation.

Nanomaterials

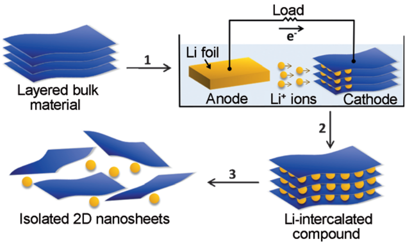

Properly piled up: Single-layer 2D semiconducting nanomaterials of MoS_2, WS_2, TiS_2, TaS_2, ZrS_2, and graphene were fabricated through an electrochemical lithiation process (see picture). The production of single-layer MoS_2 was achieved in 92% yield. A single-layer MoS_2-based thin-film transistor was fabricated, which was used for sensing NO at a detection limit of 190 ppt.

C–H Activation

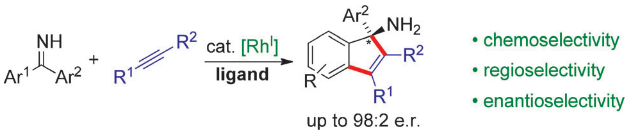

Triple selectivity: Highly substituted indenylamines can be obtained with high enantioselectivity by formal [3+2] additions of aryl ketimines with internal alkynes. These rhodium(I)-catalyzed processes proceed by selective C–H activation of one of the two arene substituents, regioselective carbometalation of the alkyne, and enantioselective addition across the imine.

Contents

Polycycles

D. T. Chase, A. G. Fix, B. D. Rose,
C. D. Weber, S. Nobusue, C. E. Stockwell,
L. N. Zakharov, M. C. Lonergan,
M. M. Haley* ____________ **11103 – 11106**

Electron-Accepting 6,12-Diethynylindeno[1,2-*b*]fluorenes: Synthesis, Crystal Structures, and Photophysical Properties

Acceptance is good! 2,8-Disubstituted indeno[1,2-*b*]fluorenes (see structure; TIPS = triisopropylsilyl) were synthesized and characterized. Electrochemical, optical, and computational data indicate that these electron-accepting hydrocarbons possess low-lying HOMO and LUMO energies, and gap energies that are comparable to common organic n-type semiconducting materials.

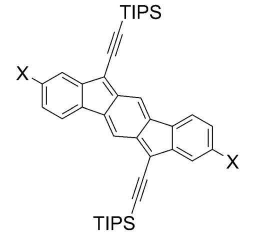

X = H, F, Cl, Br, Me, Ph, 4-$CF_3C_6H_4$, 3,5-$(CF_3)_2C_6H_3$, 2-(5-BuC_4H_2S)

Peptidomimetics

H. N. Hoang, R. W. Driver, R. L. Beyer,
A. K. Malde, G. T. Le, G. Abbenante,
A. E. Mark, D. P. Fairlie* _ **11107 – 11111**

Protein α-Turns Recreated in Structurally Stable Small Molecules

α-Turn mimics: α-Turns in proteins vary in three sets of (ϕ, ψ) angles that determine peptide backbone shape and helical pitch. Structures of cyclic tetrapeptides **1** and **2** are shown to closely match two α-turn types that are structurally influential at key sites in 20 proteins described. NMR and CD spectroscopy as well as MD simulations have been used to characterize these first examples of non-helical α-turns created in small molecules.

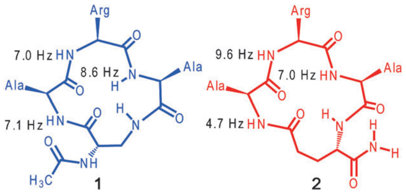

Synthetic Methods

M. Bergeron, T. Johnson,
J.-F. Paquin* ____________ **11112 – 11116**

The Use of Fluoride as a Leaving Group: S_N2' Displacement of a C–F Bond on 3,3-Difluoropropenes with Organolithium Reagents To Give Direct Access to Monofluoroalkenes

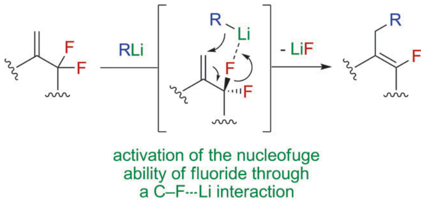

Lithium is the key to activate the nucleofuge ability of fluoride in the title transformation (see scheme). This simple and straightforward approach not only provides a practical synthetic method for the preparation of monofluoroalkenes, an important fluorinated motif, but also demonstrates the ability of fluoride to act as a competent leaving group in nucleophilic substitution reactions.

Isotopic Labeling

L. S. Campbell-Verduyn, L. Mirfeizi,
A. K. Schoonen, R. A. Dierckx,
P. H. Elsinga,*
B. L. Feringa* ____________ **11117 – 11120**

Strain-Promoted Copper-Free "Click" Chemistry for ^{18}F Radiolabeling of Bombesin

Click for PET: The GRP-receptor-specific peptide bombesin, which is often used for nuclear imaging of tumors, can be labeled with ^{18}F in a mild and rapid manner by using a copper-free azide–alkyne "click" reaction. A range of azides can be used to provide peptides with different hydrophobicities. The resulting ^{18}F radiopharmaceutical tracers (see scheme) maintain their high affinity for the targeted receptor in vitro in human prostate cancer cells.

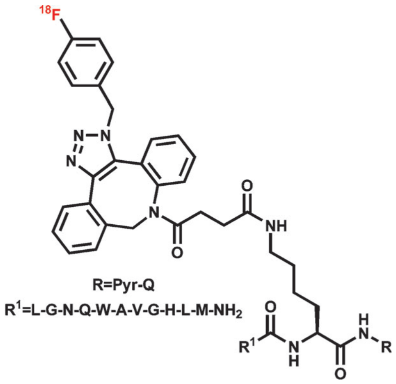

R=Pyr-Q
R^1=L-G-N-Q-W-A-V-G-H-L-M-NH_2

Hosomi–Sakurai Reaction

Y.-Y. Huang, A. Chakrabarti, N. Morita, U. Schneider, S. Kobayashi* ______ 11121 – 11124

A Catalytic Asymmetric Borono Variant of Hosomi–Sakurai Reactions with N,O-Aminals

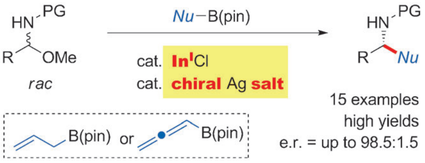

Aminal attraction: The combination of indium(I) chloride and a chiral silver binol phosphate provides an excellent catalyst for asymmetric Hosomi–Sakurai reactions between N,O-aminals and boronates (see scheme; PG = protecting group, pin = pinacolato). The substrate scope includes aromatic, heteroaromatic, and aliphatic N,O-aminals as well as allyl and allenyl boronates.

Cobalt-Catalyzed Cyclizations

M. E. Weiss, L. M. Kreis, A. Lauber, E. M. Carreira* ______ 11125 – 11128

Cobalt-Catalyzed Coupling of Alkyl Iodides with Alkenes: Deprotonation of Hydridocobalt Enables Turnover

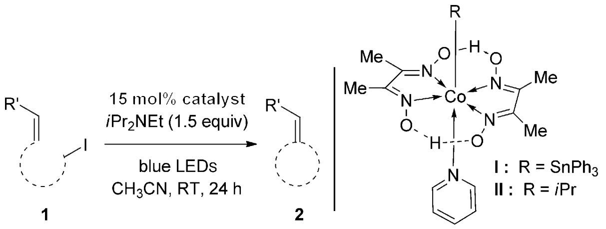

Completing the cycle: Cobalt complexes **I** and **II** were found to catalyze intramolecular alkyl Heck-type coupling reactions of alkyl iodides to alkenes upon irradiation with visible light in the presence of a tertiary amine base. The use of base is key to the catalytic turnover. The compatibility of the method with a broad range of functional groups opens opportunities for synthesis.

Dioxygen Activation

S. Paria, L. Que,, Jr.,* T. K. Paine* ______ 11129 – 11132

Oxidative Decarboxylation of Benzilic Acid by a Biomimetic Iron(II) Complex: Evidence for an Iron(IV)–Oxo–Hydroxo Oxidant from O_2

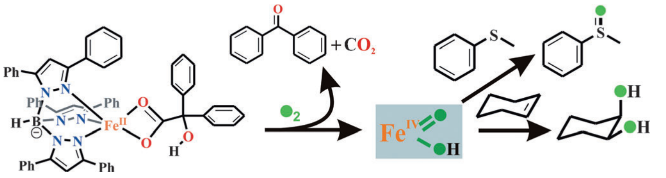

O_2-dependent transformation: An iron(II)-benzilate complex of a tridentate N3 donor ligand reacts with O_2 to undergo oxidative decarboxylation. Cyclohexene is selectively converted into *cis*-cyclohexane-1,2-diol in the reaction.

Homogeneous Catalysis

S. Y. Cai, Z. Liu, W. B. Zhang, X. Y. Zhao, D. Z. Wang* ______ 11133 – 11137

Gold-Catalyzed [3+2] Cycloaddition/Hydrolytic Michael Addition/Retro-Aldol Reactions of Propargylic Esters Tethered to Cyclohexadienones

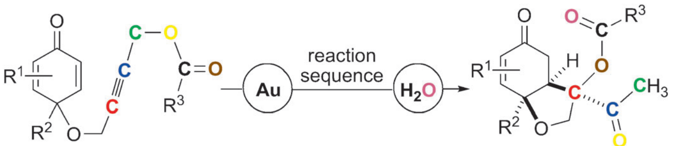

A golden dance! A series of symmetric and nonsymmetric propargylic esters tethered to cyclohexadienones were found to undergo the title reaction sequence under mild reaction conditions through gold catalysis. The product cyclohexenones or cyclohexanones having a γ-quaternary center arise from simultaneous multiatom transpositions with complete stereochemical control.

Contents

MOFs at High Pressure

A. J. Graham, D. R. Allan, A. Muszkiewicz,
C. A. Morrison,
S. A. Moggach* ________ **11138–11141**

The Effect of High Pressure on MOF-5: Guest-Induced Modification of Pore Size and Content at High Pressure

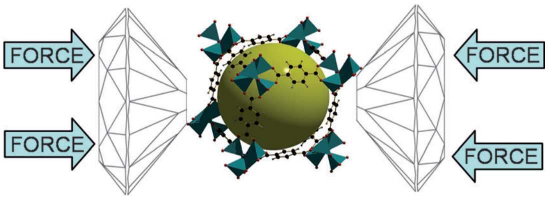

Grace under pressure: In the first high-pressure crystallographic study on the metal–organic framework MOF-5, increasing pressure initially results in the pressure-transmitting fluid being squeezed into the pores. Further pressure increase causes a large reduction in pore content as solvent is evacuated from the pores, until a complete loss of crystallinity is observed at pressures above 3.2 GPa.

Cross-Coupling

X.-F. Wu, H. Neumann,
M. Beller* ____________ **11142–11146**

Convenient and General Palladium-Catalyzed Carbonylative Sonogashira Coupling of Aryl Amines

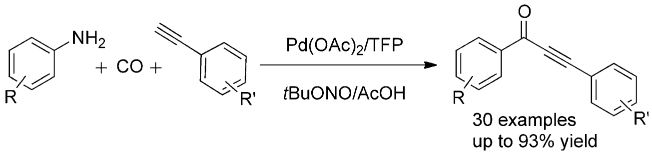

Bar (alky)none: A general and efficient method for carbonylative Sonogashira coupling reactions of anilines to generate alkynones has been developed (see scheme; TFP = tri(2-furyl)phosphine). The reaction proceeds under mild conditions and no base is needed.

Computational Chemistry

G. Kovács, A. Lledós,*
G. Ujaque* ____________ **11147–11151**

Hydroamination of Alkynes with Ammonia: Unforeseen Role of the Gold(I) Catalyst

Putting two and two together: Two key factors were found to account for the efficiency of the gold(I)/ligand catalyst in the hydroamination of alkynes with ammonia. On one hand, the excess nucleophile, NH_3, assists in the proton transfer, and on the other an unforeseen [Au] migration allows a feasible enamine–imine tautomerization.

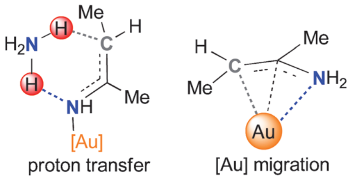

Homogeneous Catalysis

X. Xu, W. Hu, P. Y. Zavalij,
M. P. Doyle* ___________ **11152–11155**

Divergent Outcomes of Carbene Transfer Reactions from Dirhodium- and Copper-Based Catalysts Separately or in Combination

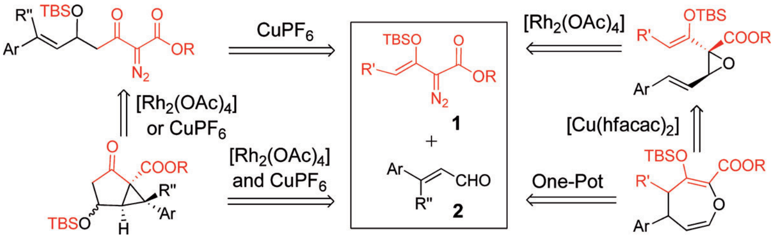

Divergent catalysis: The use of copper and rhodium catalysts separately or in combination directs reactions between vinyldiazoacetates **1** and cinnamaldehydes **2** from formal [4+3] cycloaddition (epoxidation followed by Cope rearrangement), to intramolecular cyclopropanation, to Mukaiyama-aldol reactions. The reactions proceed selectively and in high yield.

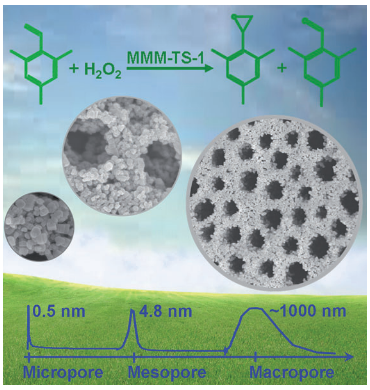

Quasi-solid-state crystallization was used to prepare zeolite TS-1 catalysts with micro–meso–macroporous (MMM) structure (see picture) and improved stability. They show a well-defined macroporous structure and an interconnected mesoporous network made of uniform zeolite TS-1 nanocrystals. The hierarchical pore structure and high stability result in superior catalytic activity in the epoxidation of larger molecules such as 2,4,6-trimethylstyrene.

Zeolites

L.-H. Chen , X.-Y. Li, G. Tian, Y. Li,
J. C. Rooke, G.-S. Zhu, S.-L. Qiu,
X.-Y. Yang,* B.-L. Su* ____ **11156 – 11161**

Highly Stable and Reusable Multimodal Zeolite TS-1 Based Catalysts with Hierarchically Interconnected Three-Level Micro–Meso–Macroporous Structure

---

Highly occupied: A highly porous form of $Mg(BH_4)_2$ (see picture; Mg green, BH_4 blue, unit cells shown in red) reversibly absorbs H_2, N_2, and CH_2Cl_2. At high pressures, this material transforms into an interpenetrated framework that has 79% higher density than the other polymorphs. $Mg(BH_4)_2$ can act as a coordination polymer that has many similarities to metal–organic frameworks.

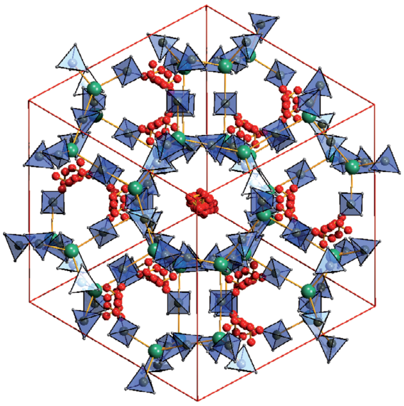

Hydrogen Storage

Y. Filinchuk,* B. Richter, T. R. Jensen,*
V. Dmitriev, D. Chernyshov,
H. Hagemann ____ **11162 – 11166**

Porous and Dense Magnesium Borohydride Frameworks: Synthesis, Stability, and Reversible Absorption of Guest Species

---

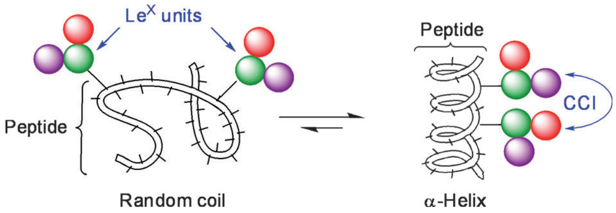

Probing weak interactions: A peptide random-coil:α-helix equilibrium has been used to identify a weak carbohydrate–carbohydrate interaction (CCI). Glucose and lactose destabilized the helical conformer while Lewis^X trisaccharide led to increased helicity. Though small, the trend observed indicates that this peptide reporter can detect a single CCI in isolation.

Carbohydrates

T. M. Altamore, C. Fernández-García,
A. H. Gordon, T. Hübscher,
N. Promsawan, M. G. Ryadnov, A. J. Doig,
D. N. Woolfson,*
T. Gallagher* ____ **11167 – 11171**

Random-Coil:α-Helix Equilibria as a Reporter for the Lewis^X–Lewis^X Interaction

---

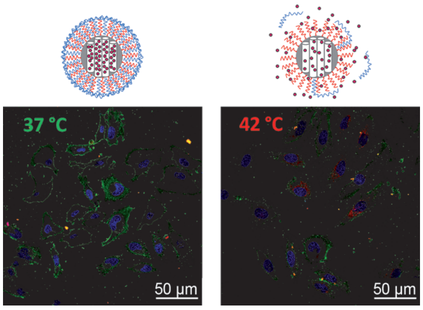

Trapped: Mesoporous silica nanoparticles were loaded with a fluorescent guest and functionalized with octadecyltrimethoxysilane. The alkyl chains interact with paraffins, which build a hydrophobic layer around the particle (see picture). Upon melting of the paraffin, the guest molecule is released, as demonstrated in cells for the guest doxorubicin. The release temperature can be tuned by choosing an appropriate paraffin.

Molecular Gates

E. Aznar, L. Mondragón, J. V. Ros-Lis,
F. Sancenón, M. D. Marcos,
R. Martínez-Máñez,* J. Soto,
E. Pérez-Payá, P. Amorós **11172 – 11175**

Finely Tuned Temperature-Controlled Cargo Release Using Paraffin-Capped Mesoporous Silica Nanoparticles

Electrochemical DNA Sensor

K. Hsieh, R. J. White, B. S. Ferguson,
K. W. Plaxco, Y. Xiao,*
H. T. Soh* ______________ 11176 – 11180

Polarity-Switching Electrochemical Sensor for Specific Detection of Single-Nucleotide Mismatches

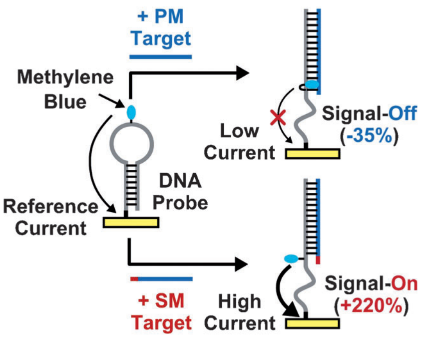

Getting a response: A surface-bound and redox-modified (methylene blue) DNA probe architecture is at the heart of a sensor for detecting single-nucleotide mismatched targets with a "polarity-switching" response. It outputs a decreased Faradaic current when hybridized to a perfectly matched (PM) target, and an increased Faradaic current when hybridized to a single-base mismatched (SM) target (see scheme).

Chemically Defined Differentiation

R. Gonzalez, J. W. Lee,
P. G. Schultz* ___________ 11181 – 11185

Stepwise Chemically Induced Cardiomyocyte Specification of Human Embryonic Stem Cells

Cellular differentiation: Using a high-throughput imaged-based screen a chemical cocktail that promotes efficient human pluripotent cells (hESCs) differentiation into cardiomyocytes was identified.

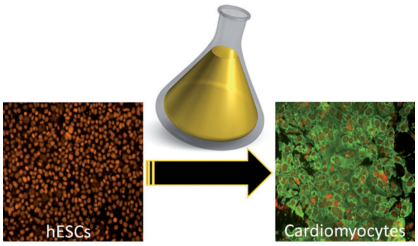

Peptide Crystallization

X. Yan,* Y. Su, J. Li,* J. Früh,
H. Möhwald ____________ 11186 – 11191

Uniaxially Oriented Peptide Crystals for Active Optical Waveguiding

Riding the waves: An aldehyde triggers oriented long-range crystallization of self-assembling fibrous diphenylalanine peptide networks (see picture). The crystal growth is self-adjustable and likely subject to kinetic regulation, which leads to the 3D confinement of uniaxially oriented substructures in the resultant crystal. The peptide crystals exhibit remarkable thermal stability and optical waveguiding properties.

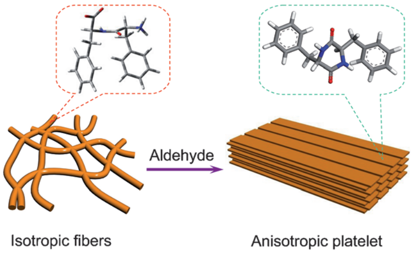

Self-Powered Nanodevice

C. Pan, Z. Li, W. Guo, J. Zhu,
Z. L. Wang* ____________ 11192 – 11196

Fiber-Based Hybrid Nanogenerators for/as Self-Powered Systems in Biological Liquid

Electrifying: A fiber-based hybrid nanogenerator for simultaneous or independent harvesting of mechanical and biochemical energy is presented. The hybrid system consists of a nanogenerator (FNG) and a biofuel cell (FBFC) and provides a peak output of 3.1 V and 200 nA. It also serves as a self-powered sensor for the quantification of pressure variations.

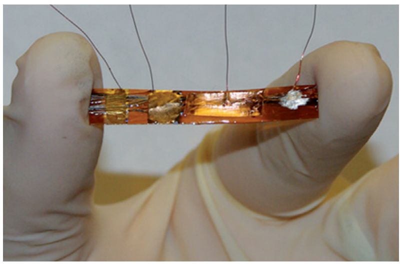

Catalytic Amination

M. Zhang, S. Imm, S. Bähn, H. Neumann,
M. Beller* ______________ 11197 – 11201

Synthesis of α-Amino Acid Amides: Ruthenium-Catalyzed Amination of α-Hydroxy Amides

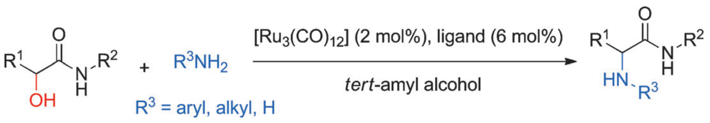

Give me an N: The catalytic amination of α-hydroxy amides with a variety of amines, including anilines, primary and secondary aliphatic amines, and ammonia, yields a wide range of α-amino amides (see scheme). This atom-efficient amination protocol proceeds efficiently in the presence of a commercially available $[Ru_3(CO)_{12}]$/DCPE catalyst system.

Fuel Cells

T. Matsumoto, K. Kim,
S. Ogo* ______ **11202 – 11205**

Molecular Catalysis in a Fuel Cell

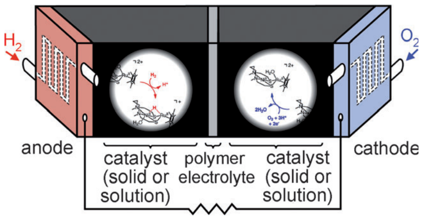

Jack of all trades: A fuel cell based on a single molecular catalyst (see picture) uses a [NiFe]hydrogenase mimic to catalyze the oxidation of H_2. Crucially, the catalyst is also active for the reduction of O_2, allowing the construction of a fully functional fuel cell. This molecular catalyst can function both in solid and solution phases, allowing precise observation of the mechanism.

Caged Fluorophores

L. M. Wysocki, J. B. Grimm,
A. N. Tkachuk, T. A. Brown, E. Betzig,
L. D. Lavis* ______ **11206 – 11209**

Facile and General Synthesis of Photoactivatable Xanthene Dyes

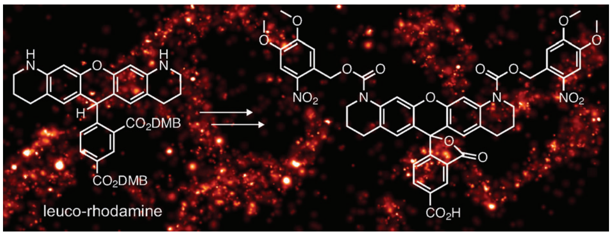

Despite the apparent simplicity of the xanthene fluorophores, the preparation of caged derivatives with free carboxy groups remains a synthetic challenge. A straightforward and flexible strategy for preparing rhodamine and fluorescein derivatives was developed using reduced, "leuco" intermediates.

Ubiquitin Chains

C. A. Castañeda, L. Spasser, S. N. Bavikar,
A. Brik,* D. Fushman* ______ **11210 – 11214**

Segmental Isotopic Labeling of Ubiquitin Chains To Unravel Monomer-Specific Molecular Behavior

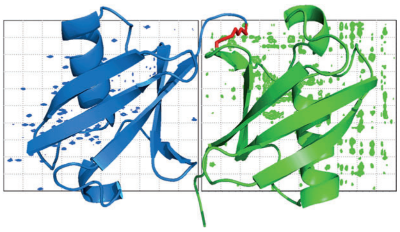

"Seeing" each monomer in ubiquitin chains: By combination of the chemical synthesis of one ubiquitin monomer with recombinant expression of its ^{15}N-containing counterpart, the labeling of ubiquitins in non-enzymatically assembled di-ubiquitin chains was achieved, to enable monomer-specific studies in solution. This allowed the first characterization of the structure, dynamics, intrachain interactions, and ligand binding of Lys33-linked di-ubiquitin.

Protein Screening

T. W. Kim, H. A. Chokhawala, M. Hess,
C. M. Dana, Z. Baer, A. Sczyrba,
E. M. Rubin, H. W. Blanch,*
D. S. Clark* ______ **11215 – 11218**

High-Throughput In Vitro Glycoside Hydrolase (HIGH) Screening for Enzyme Discovery

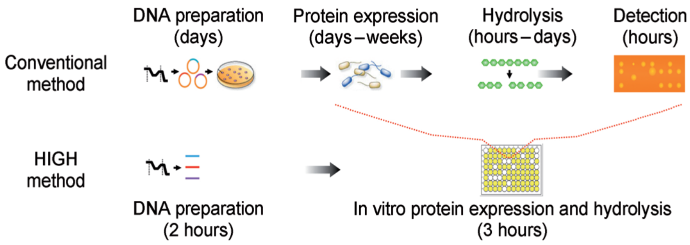

Combined efforts: A high-throughput protein-expression and screening method (HIGH method, see picture) provides a rapid approach to the discovery of active glycoside hydrolases in environmental samples. HIGH screening combines cloning, protein expression, and enzyme hydrolysis in one pot; thus, the entire process from gene expression to activity detection requires only three hours.

Extended CO_2 Carbonates

C.-S. Yoo,* A. Sengupta,
M. Kim ______________ **11219 – 11222**

Carbon Dioxide Carbonates in the Earth's Mantle: Implications to the Deep Carbon Cycle

Under pressure: An increase in the ionic character in C–O bonds at high pressures and temperatures is shown by the chemical/phase transformation diagram of CO_2 (see picture). The presence of carbonate carbon dioxide (i-CO_2) near the Earth's core–mantle boundary condition provides insights into both the deep carbon cycle and the transport of atmospheric CO_2 to anhydrous silicates in the mantle and iron core.

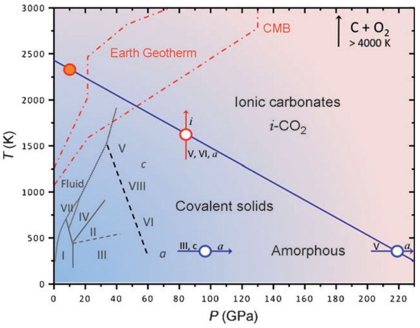

Single-Molecule Electronics

M. L. Perrin, F. Prins, C. A. Martin,
A. J. Shaikh, R. Eelkema, J. H. van Esch,
T. Briza, R. Kaplanek, V. Kral,
J. M. van Ruitenbeek,
H. S. J. van der Zant,
D. Dulić* ______________ **11223 – 11226**

Influence of the Chemical Structure on the Stability and Conductance of Porphyrin Single-Molecule Junctions

Different bridging geometries can explain the observation that porphyrin molecules with added thiol end groups and pyridine axial groups form more-stable single-molecule junctions with an increased spread in low-bias conductance. The stability of these geometries is demonstrated by time-dependent conductance measurements. In contrast, rodlike molecules show one preferential binding geometry.

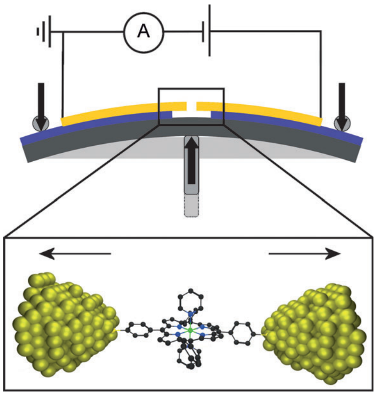

Rare-Earth-Metal Complexes

Y. D. Lv, X. Xu, Y. F. Chen,* X. B. Leng,
M. V. Borzov ______________ **11227 – 11229**

Well-Defined Soluble P^{3-}-Containing Rare-Earth-Metal Compounds

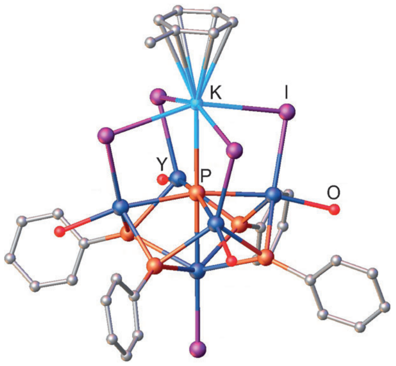

A rare find: Soluble P^{3-}-containing rare-earth-metal coordination compounds have been synthesized. A P^{3-}-containing polymetallic yttrium iodide was obtained through P–Si (or H) and P–C bond cleavage, and this compound can be transferred into other P^{3-}-containing yttrium coordination compounds by metathesis reactions.

Zeolites

A. Mayoral,* T. Carey, P. A. Anderson,
A. Lubk, I. Diaz ______________ **11230 – 11233**

Atomic Resolution Analysis of Silver Ion-Exchanged Zeolite A

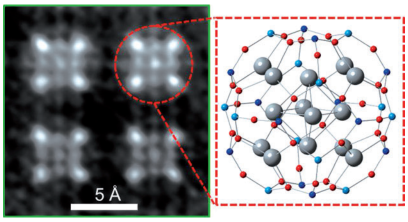

The three-dimensional structure of Ag ion-exchanged zeolite A was studied by XRD and scanning transmission electron microscopy. Despite the difficulties in the microscopic investigation of zeolites with high Al content, the arrangement of isolated Ag ions and Ag clusters of six atoms was visualized (see picture).

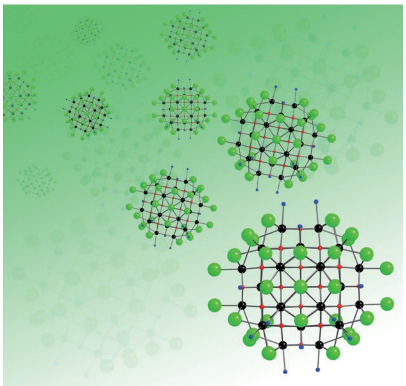

Oil and vinegar: Colloidal plutonium is an important component of Pu aqueous speciation. Pu colloids are problematic in nuclear separations and are a potential transport vector in the environment. Using a mixture of *n*-octanol and trichloroacetic acid a selective and reversible separation of these particles can be achieved by exploiting their surface reactivity. Picture: $Li_2[Pu_{38}O_{56}Cl_{42}(H_2O)_{20}]\cdot 15\,H_2O$.

Actinides

R. E. Wilson,* S. Skanthakumar,
L. Soderholm ______ **11234–11237**

Separation of Plutonium Oxide Nanoparticles and Colloids

Selection with modified aptamers: A method is described for design of glycocluster ligands by directed evolution. Glycan azides are attached to a library of alkyne-containing DNA sequences. DNA sequences which cluster the glycans best for multivalent binding to the target are selected and amplified. This method has been applied to the development of high-mannose clusters which bind HIV-neutralizing antibody 2G12.

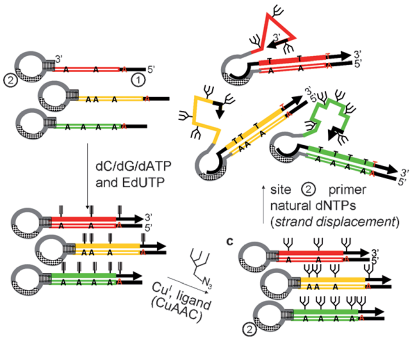

DNA-Scaffolded Glycoclusters

I. S. MacPherson, J. S. Temme,
S. Habeshian, K. Felczak, K. Pankiewicz,
L. Hedstrom,*
I. J. Krauss* ______ **11238–11242**

Multivalent Glycocluster Design through Directed Evolution

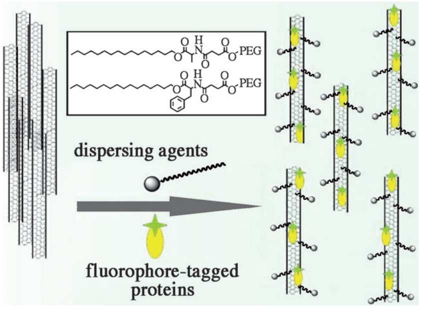

Designed to deliver: Carbon nanotube (CNT)/amphiphile hybrids with remarkable stability and cell viability under biologically relevant conditions can be obtained by rational modification of the molecular structure of amphiphilic dispersing agents (see scheme; PEG = poly(ethylene glycol)). The CNT/amphiphile hybrids are dispersible in water and efficiently shuttle proteins across mammalian cell membranes.

Nanotubes

S. Brahmachari, D. Das, A. Shome,
P. K. Das* ______ **11243–11247**

Single-Walled Nanotube/Amphiphile Hybrids for Efficacious Protein Delivery: Rational Modification of Dispersing Agents

---

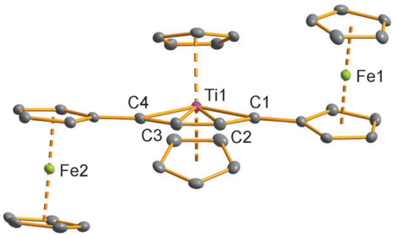

C_2 and C_4 with three metallocenes: Two diferrocenyl-substituted three- and five-membered titanacycles (see structure) were synthesized. Their molecular structures in the solid state reveal symmetrically arranged metallocene groups connected only by a C_2 or C_4 chain. For the first time, the electrochemical behavior of these systems was studied and a linearization of the ligand in the dication of the five-membered ring was observed.

Oligocyclopentadienyl Complexes

K. Kaleta, A. Hildebrandt, F. Strehler,
P. Arndt, H. Jiao, A. Spannenberg,
H. Lang,* U. Rosenthal* _ **11248–11252**

Ferrocenyl-Substituted Metallacycles of Titanocenes: Oligocyclopentadienyl Complexes with Promising Properties

Contents

Cage Compounds

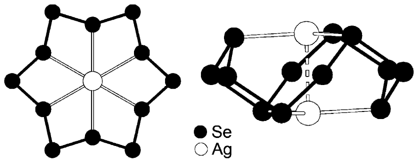

Foreshadowing a new selenium modification …? Upon treatment of red, amorphous selenium with the silver salts of two large weakly coordinating anions (WCA), the thermodynamically driven formation of $[Ag_2Se_{12}]^{2+}$ occurred. The structure of the dication is an unprecedented D_{3d}-symmetric 14-vertex cage built from six six-membered rings in a boat conformation that includes a weak argentophilic Ag–Ag bond.

Asymmetric Catalysis

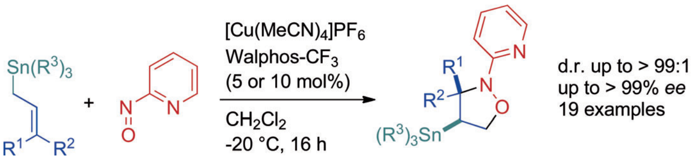

Click! Formal [3+2] cycloadditions of 2-nitrosopyridine with various allylstannanes give 4-stannyl-substituted isoxazolidines. The use of $[Cu(MeCN)_4]PF_6$, in combination with a Walphos ligand, leads to excellent enantioselectivies and high yields. With *cis*-2-alkenylstannanes as nucleophiles, 3-alkyl-4-stannyl-substituted isoxazolidines are formed with excellent diastereo- and enantioselectivities.

Supporting information is available on www.angewandte.org (see article for access details).

A video clip is available as Supporting Information on www.angewandte.org (see article for access details).

This article is available online free of charge (Open Access).

Service